Electronic Supplementary Material (ESI) for Materials Horizons

Supporting Information

Self-Assembly of Aligned Rutile@Anatase TiO_2 Nanorod@CdS Quantum Dots Ternary Core-Shell Heterostructure: Cascade Electron-Transfer by Interfacial Design

*Fang-Xing Xiao, Jianwei Miao, Bin Liu**

School of Chemical and Biomedical Engineering, Nanyang Technological University, 62 Nanyang Drive, Singapore 637459, Singapore. Fax: (65) 6794-7553; Tel: (65) 6513-7971;

E-mail:liubin@ntu.edu.sg

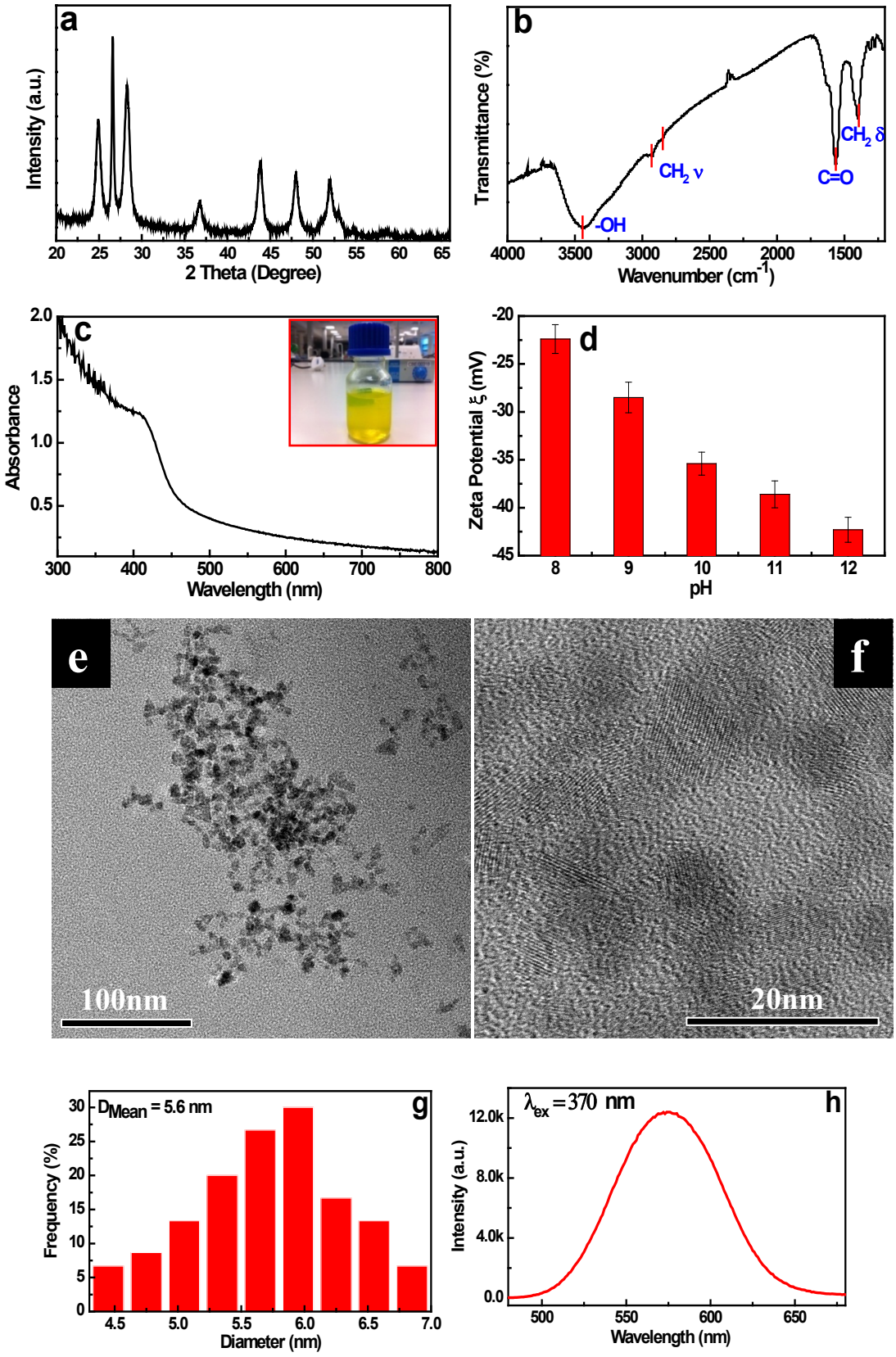

Figure S1. (a) XRD pattern, (b) FTIR, (c) UV-vis spectrum, (d) zeta potential, (e & f) TEM images, (g) mean diameter histogram and (h) fluorescence spectrum of CdS@TGA QDs.

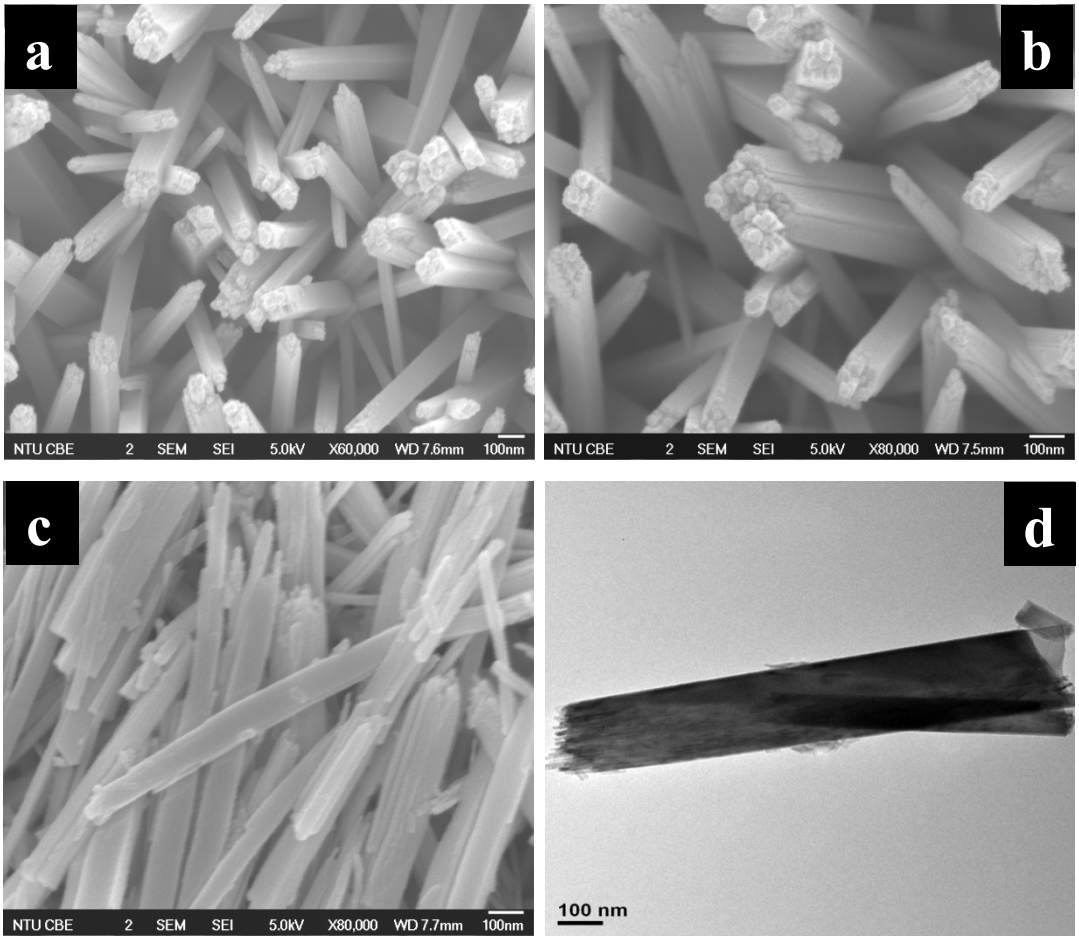

Figure S2. (a-c) Detailed FESEM images of original rutile TiO_2 NRs on FTO substrate, (d) TEM image of a single rutile TiO_2 NR.

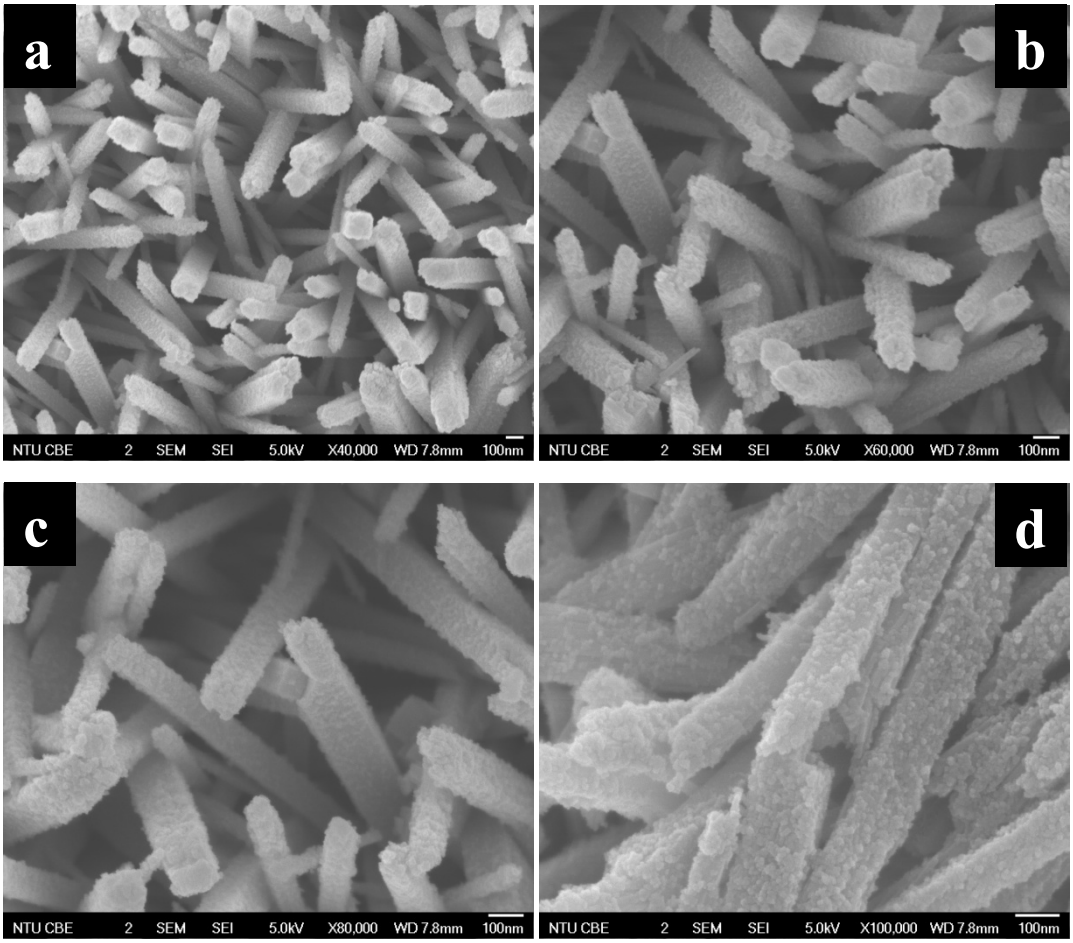

Figure S3. Detailed FESEM images of rutile@anatase TiO_2 NRs (TN) binary core-shell heterostruture on FTO substrate.

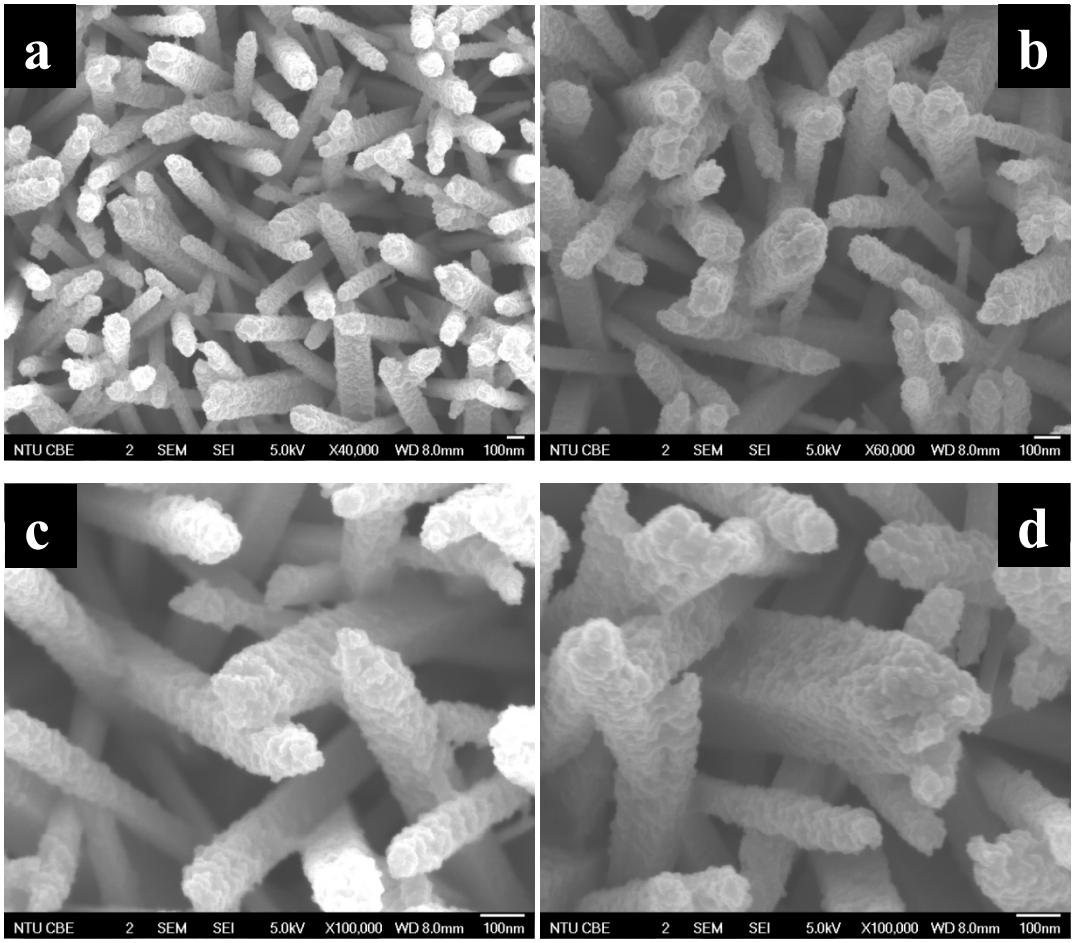

Figure S4. Detailed FESEM images of rutile@anatase TN@CdS QDs ternary core-shell heterostructure on FTO substrate.

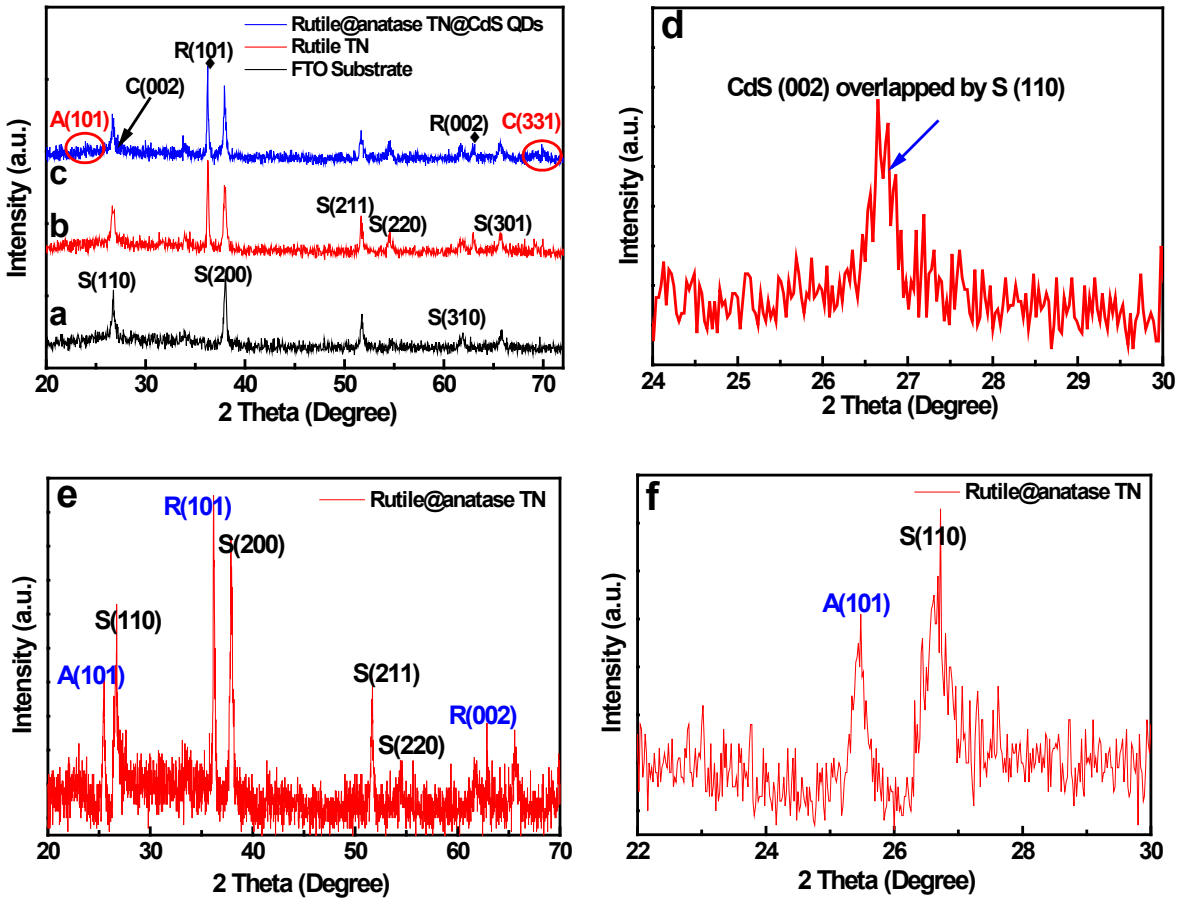

Figure S5. XRD patterns of (a) FTO substrate, (b) rutile TiO_2 NRs and (c) rutile@anatase TN@CdS QDs ternary core-shell heterostructure, (d) enlargement of the spectrum shown in curve c. (e) XRD pattern of rutile@anatase TN, and (f) enlargement of the spectrum shown in curve e. (*It should be pointed out that in order to amplify the signal of anatase TiO_2, more precursor was deposited on the rutile nanorods and subjected to the same treatment.*) (A: anatase, R: rutile, C: CdS, F: FTO substrate).

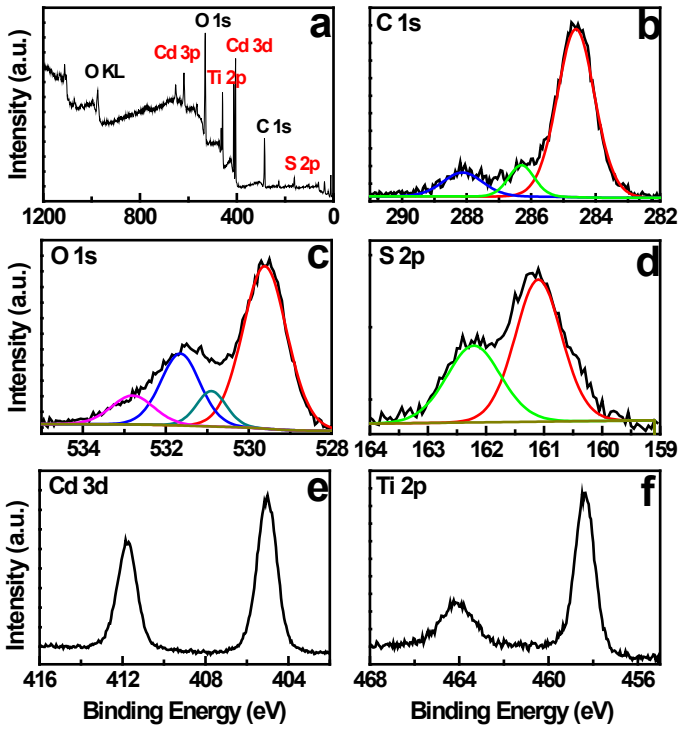

Figure S6. (a) Survey and high-resolution XPS spectra of (b) C 1s, (c) O 1s, (d) S 2p, (e) Cd 3d and (f) Ti 2p for rutile@anatase TN@CdS QDs ternary core-shell heterostructure.

Table S1. Chemical species *versus* binding energy for rutile@anatase TN@CdS QDs ternary core-shell heterostructure.

Element	*Rutile@anatase TN@CdS QDs*	*Chemical Bond Species*
C 1s A	284.61	C-C/C-H
C 1s B	286.30	C-OH/C-O-C[1]
C 1s C	288.20	Carboxylate (CO_3^{2-})[2]
O 1s A	529.61	Lattice Oxygen
O 1s B	530.90	Ti-OH[3]
O 1s C	531.65	C-OH/C-O-C
O 1s D	532.80	COOH
Ti $2p_{3/2}$	458.35	Anatase (4^+)[4]
Ti $2p_{1/2}$	464.10	Anatase (4^+)
Cd $3d_{5/2}$	405.03	Cd (2^+)[5]
Cd $3d_{3/2}$	411.76	Cd (2^+)
S $2p_{3/2}$	161.15	S (2^-)[6]

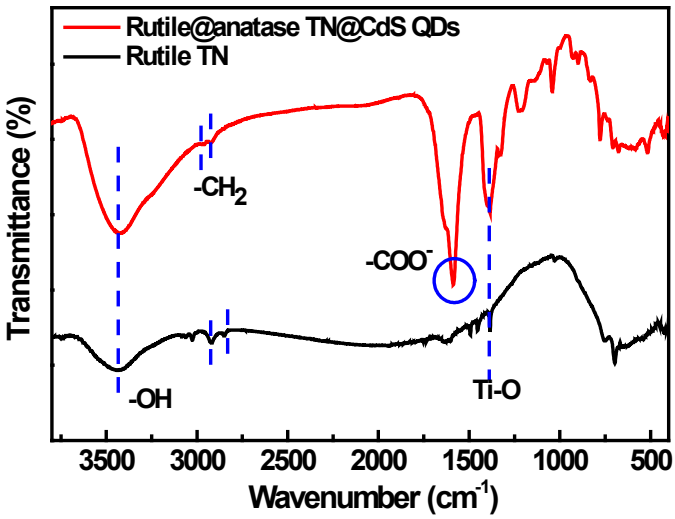

Figure S7. Fourier transformed infrared (FTIR) spectra of (a) rutile TiO_2 NRs and (b) rutile@anatase TN@CdS QDs ternary core-shell heterostructure.

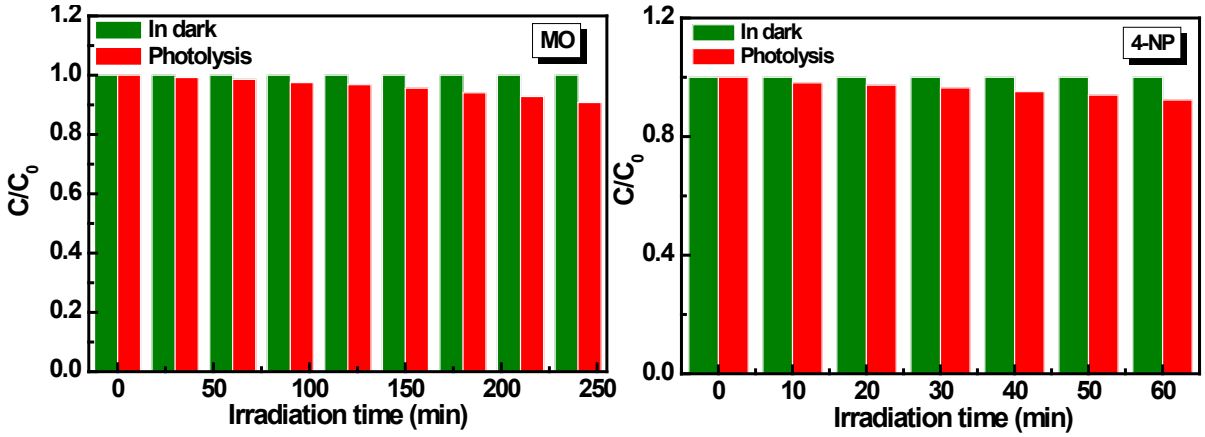

Figure S8. Blank experiments for photocatalytic degradation of (a) MO and (b) selective photocatalytic reduction of 4-NP without light or without catalyst.

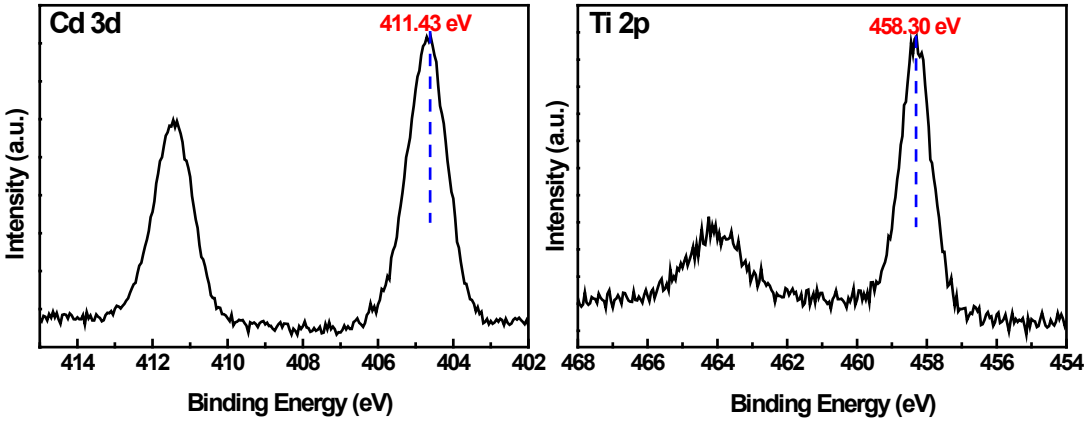

Figure S9. High-resolution XPS spectra of Cd 3d and Ti 2p for rutile@anatase TN@CdS QDs ternary core-shell heterostructure after photocatalytic reactions.

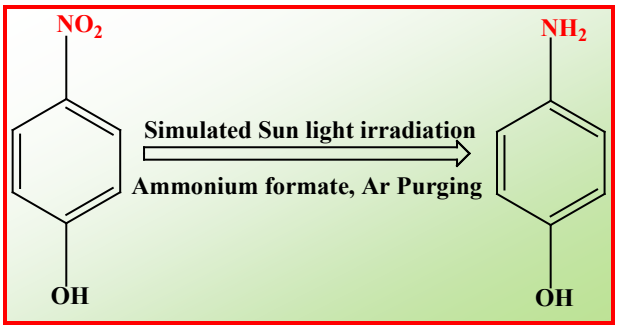

Figure S10. Schematic illustration of selective photocatalytic reduction of 4-NP to 4-AP under experimental conditions.

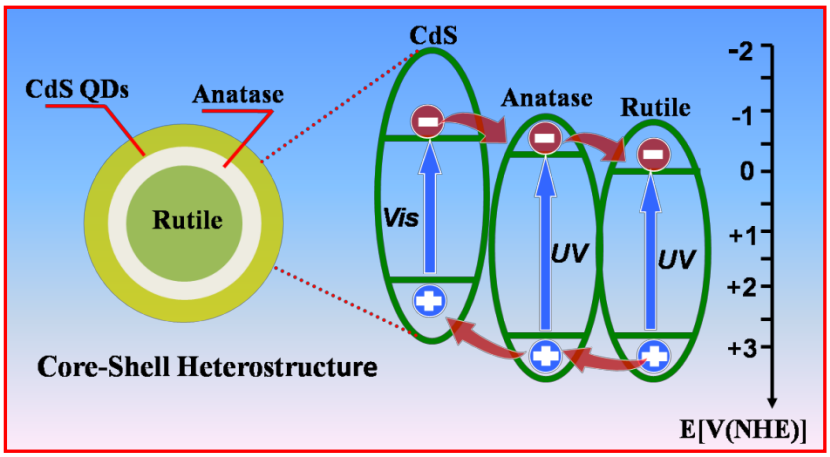

Figure S11. Schematic diagram representing the photocatalytic mechanism of the rutile@anatase TN@CdS QDs ternary core-shell heterostructure.

Experimental section

1. Materials

Fluorine-doped tin oxide (FTO), deionized water (DI H_2O, Milipore, 18.2 MΩ·cm resistivity), hydrochloric acid (HCl), thioglycolic acid ($C_2H_4O_2S$, TGA), cadmium chloride ($CdCl_2$. $2.5H_2O$), sodium sulfide (Na_2S. $9H_2O$), sodium hydroxide (NaOH), titanium butoxide, titanium (IV) bis(ammonium lactate) dihydroxide (TALH), poly(diallyldimethylammonium chloride) (PDDA), 3-aminopropyl-trimethoxysilane (APS), ethanol (C_2H_6O), ammonium formate ($HCOONH_4$), 4-nitrophenol.

2. Prepaation of TiO_2 nanorods

TiO_2 nanorod arrays (TiO_2 NRs) on transparent conductive FTO substrate were synthesized by a hydrothermal growth method according to our previous work.[7] In a typical synthesis, FTO substrates were first cleaned with acetone, ethanol, and DI H_2O for 5 min, respectively, and then dried by N_2 stream. The precursor was prepared by adding 0.45 mL of titanium butoxide (97 %, Aldrich) to a well-mixed solution containing 15 mL of HCl and 15 mL of DI H_2O, and then the whole mixture was stirred for another 10 min until the solution became clear. Afterwards, the precursor solution was poured into a Teflon-liner stainless autoclave (50 mL) with the FTO substrates placed at an angle against the wall with the conductive side facing down. Hydrothermal growth was conducted at 150 ^oC for 12 h in an electric oven. Finally, the FTO substrate were rinsed with DI H_2O and dried in ambient air.

3. Preparation of CdS quantum dots (QDs)

CdS QDs were synthesized according to previous reports with slight modification.[8,9] Briefly, 250 μL of thioglycolic acid (TGA) was added to 50 mL of $CdCl_2$ (1.0×10^{-2} M) aqueous solution and N_2 was bubbled throughout the solution for 30 min to remove O_2 at 110 ^oC. During this period, 1.0 M NaOH was dropwisely added to adjust the solution pH to 8. Then, 5.5 mL of 0.1 M Na_2S aqueous solution was rapidly injected to grow TGA-capped water-soluble CdS QDs, and the reaction mixture was continuously refluxed under N_2 atmosphere for 4 h. This procedure produced CdS QDs with a Cd to S ratio of 1: 1.1. Finally, the desired TGA-stabilized CdS QDs were stored in a refrigerator at 4 ^oC for further use.

4. Prepaation of rutile@anatase TN@CdS QDs ternary core-shell heterostructure

TiO_2 NRs were dipped into PDDA aqueous solution (1 mg/mL, 0.5 M NaCl, pH = 8) for 20 min, rinsed with DI H_2O and dried with N_2 stream, and subsequently dipped into TALH aqueous solution (5 wt %) for another 20 min, rinsed with DI H_2O and dried with N_2 flow. The TALH-treated TiO_2 NRs was refluxed in 50 mL of DI H_2O for 24 h. The samples obtained after refluxing were dried by a N_2 flow and subjected to calcination (450 ^oC, 1h, in air). Then, the samples were refluxed in a mixed solution containing ethanol (50 mL) and APS (500 µL) for 4 h. Afterwards, the APS-modified samples were washed sufficiently with ethanol to remove residual APS, dried with a N_2 flow, and dipped into CdS QDs aqueous solution for 20 min to trigger the self-assembly deposition under ambient conditions. Eventually, the samples were completely dried at 80 ^oC for 30 min. For comparison, rutile@CdS QDs binary nanocomposite in which CdS QDs was directly deposited on the APS-modified rutile TiO_2 NRs, *i.e.* without intermediate anatase TiO_2 layer, was also prepared under similar experimental conditions.

5. Characterization

The phase composition was determined by X-ray diffraction (XRD) on a Bruker D8 Advance X-ray diffractometer with Cu Kα radiation. The accelerating voltage and applied current were 40 kV and 40 mA, respectively. Transmission electron microscopy (TEM) and high-resolution transmission electron microscopy (HRTEM) images were obtained by a JEOL model JEM 2010 EX instrument at an accelerating voltage of 200 kV. The nanorods were carefully scratched from the FTO substrate using a blade and dispersed in 5 mL of ethanol with the aid of ultrasonication (Elmasonicator 30 H) for 10 minutes, and then dropwisely added onto carbon coated Cu-grid for TEM measurement. The UV-vis diffuse reflectance spectra (DRS) were recorded on a Varian Cary 500 Scan UV-vis-NIR spectrometer. X-ray photoelectron spectroscopy (XPS) measurements were conducted on an ESCALAB 250 photoelectron spectrometer (Thermo Fisher Scientific) at 2.4×10^{-10} mbar using a monochromatic Al Kα X-ray beam (1486.60 eV). Binding energy (BE) of the element was calibrated to the carbon BE of 284.60 eV. The morphologies of the samples were measured by field emission scanning electron microscopy (FESEM, JEOL JSM6701F). Fourier transformed infrared (FTIR) spectra were recorded in the transmittance mode with a resolution of 4 cm^{-1} using a Perkin Elmer FTIR spectrometer. Photoelectrochemical measurements were performed on a CHI660B electrochemical workstation. The photoelectrochemical system was comprised of three electrodes, a single-compartment quartz cell which was filled with 0.1 M Na_2S electrolyte (20 mL) and a potentiostat. A platinum black sheet was used as a counter electrode with Ag/AgCl/KCl as a

reference electrode. A thin film of the sample (25 mm × 17 mm) was employed as a working electrode. A 300 W Xe arc lamp (NEWPORT) equipped with an AM 1.5 cutoff filter was used as exciting light source for light irradiation.

6. Photocatalytic performances

(a) Photocatalytic activity of the ternary core-shell heterostructure was evaluated by using methyl orange (MO) as a model organic pollutant compound. In a typical test, the samples with the same area (25 mm × 17 mm) were soaked into 15 mL of MO aqueous solution (5 mg/L, pH = 7) in a quartz cuvette (55 mm × 54 mm × 17 mm). Before irradiation, the mixtures were kept in the dark for 1 h to reach equilibrium of adsorption-desorption at room temperature. A 300 W Xe arc lamp equipped with an AM 1.5 cutoff filter was applied as light source (100 mW/cm^2). All samples were placed 20 cm away from the light source. At each irradiation time interval of 30 min, light absorption of the reaction solution was measured by a Cary 500 scan UV-Vis spectrophotometer. The concentration of MO was determined by monitoring the absorption peak at 464 nm. The degradation ratio of MO at each time interval was calculated from the ratio of the light absorbance of irradiated to the non-irradiated solution. (b) For selective photocatalytic reduction of 4-nitrophenol (4-NP), the samples were dipped into 4-NP (10 mg/L) aqueous solution in a quartz cuvette. After adding 20 mg of HCO_2NH_4, the suspension was stirred (200 rpm) in dark for 1 h to ensure establishment of adsorption-desorption equilibrium. As the reaction proceeded, the solution was taken at a certain time interval (t = 10 min) for analysis. The variation of 4-NP concentration during the reaction was analyzed by measuring characteristic peak absorbance of 4-NP at *ca.* 325 nm with UV-vis spectroscopy.[10] The whole photocatalytic reduction process was carried out under Ar bubbling.

References

1 S. Biniak, G. Szymanski, J. Siedlewski and A. Swiatkowski, *Carbon* **1997**, 35, 1799-1810.

2 X. M. Wei and H. C. Zeng, *Chem. Mater*. **2003**, 15, 433-442.

3 J. Li, S. B. Tang, L. Lu and H. C. Zeng, *J. Am. Chem. Soc*. **2007**, 129, 9401-9409.

4 O. I. Micic, M. T. Nenadovic, M. W. Peterson and A. J. Nozik, *J. Phys. Chem*. **1987**, 91, 1295-1297.

5 J. Zhang, J. G. Yu, M. Jaroniec and J. R. Gong, *Nano Lett.* **2012**, 12, 4584-4589.

6 T. Nakanishi, B. Ohtani, K. Shimazu and K. Uosaki, *Chem Phys Lett.* **1997**, 278, 233-237.

7 B. Liu, E and S. Aydil, *J. Am. Chem. Soc* .**2009**, 131, 3985-3990.

8 V. L. Colvin, A. N. Goldstein and A. P. Alivisatos, *J. Am. Chem. Soc.***1992**, 114, 5221-5230.

9 W. W. Zhao, Z. Y. Ma, P. -P. Yu, X. Y. Dong, J. -J. Xu and H. -Y. Chen, *Anal. Chem.* **2012**, 84, 917-923.

10 N. Zhang and Y. -J. Xu, *Chem. Mater.* **2013**, *25*, 1979-1988.